Volume 54
Number 38
14 October 2025
Pages 14229-14598

Dalton Transactions

An international journal of inorganic chemistry

rsc.li/dalton

ISSN 1477-9226

ROYAL SOCIETY OF CHEMISTRY

PAPER

Michal Szostak, Elwira Bisz *et al.*

IPaul^{Het} – spatially-defined, wingtip-flexible, N,C-chelating oxazole and thiazole donor N-heterocyclic carbene ligands

Dalton Transactions

ROYAL SOCIETY OF CHEMISTRY

PAPER

View Article Online
View Journal | View Issue

Check for updates

Cite this: *Dalton Trans.*, 2025, **54**, 14267

IPaul^{Het} – spatially-defined, wingtip-flexible, N,C-chelating oxazole and thiazole donor N-heterocyclic carbene ligands

Pamela Podchorodecka,[a] Błażej Dziuk,[b] Roman Szostak,[c] Michal Szostak *[d] and Elwira Bisz *[a]

N-Heterocyclic carbenes (NHCs) are among the most versatile ligands in transition metal catalysis with their steric and electronic properties playing a critical role in governing reactivity and selectivity. In this area, the wingtip unsymmetrical IPaul ligand introduced by Nelson and co-workers offers a unique balance of steric bulk and flexibility characterized by spatially-defined steric features. Herein, we report a new class of IPaul-based ligands bearing benzoxazole and benzothiazole donor wingtips. The synthesis, application, and structural and electronic characterization are described. These ligands retain the defining 'bulky yet flexible' profile of IPaul, while enabling precise control over the catalytic pocket geometry through N-heteroaryl wingtip substitution. We present their coordination chemistry with Ag(I), Pd(II), Rh(I), and Se as well as catalytic studies in cross-coupling and hydrosilylation catalyzed by Ag, Pd, and Rh complexes. By combining the steric asymmetry of IPaul with the chelating flexibility of N-azole donors, this ligand class provides stabilization of reactive metal centers and is well-suited for diverse catalytic applications. We anticipate that the combination of steric flexibility with N,C-chelation in versatile N-heterocyclic carbenes will be of broad interest across organometallic, inorganic and catalytic chemistry.

Received 4th July 2025,
Accepted 5th August 2025

DOI: 10.1039/d5dt01576f

rsc.li/dalton

Published on 06 2025. Downloaded on 06.01.2026 02:10:48.

Introduction

In the past two decades, N-heterocyclic carbenes (NHCs) have become central ligands in coordination and organometallic chemistry[1,2] due to their strong σ-donating properties and flexible steric features.[3] In particular, NHC ligands have attracted significant attention in catalysis since these ligands have been shown to stabilize highly reactive metal centers at different oxidation states, while offering a tunable steric environment around the metal center to optimize catalytic activity and selectivity.[4] Furthermore, N-heterocyclic carbenes have also found an array of key applications in functional materials, biomedicine, polymers, metal–organic frameworks, and nanoparticles, among other fields.[5,6] The broad applicability of N-heterocyclic carbenes across various chemical disciplines has been the crucial driver in considerable research efforts towards the design of new classes of N-heterocyclic carbenes. Notably, contributions by Nolan,[7] Glorius,[8] Bertrand,[9] Nelson,[10] and others[11] have successfully introduced diverse sterically-demanding N-heterocyclic carbenes, which are now widely employed in the toolbox of organometallic chemistry.

In this context, the incorporation of N-heterocyclic donors into NHC ligands adds an additional level of control by allowing chelation through heteroatoms, thus further enhancing metal stabilization *via* hemilabile coordination.[12] Recent studies have demonstrated the synthesis and structural flexibility of N,C-chelating oxazole NHC ligands, showcasing their utility in catalysis through their unique steric and electronic adaptability.[13] Specifically, oxazole-functionalized NHC ligands have been shown to feature a freely-rotatable oxazole moiety, which dynamically adjusts to the steric environment of the metal center and provides an additional chelating site, thus significantly impacting the coordination chemistry and catalytic behavior.

Simultaneously, spatially-defined steric impact has emerged as a compelling strategy in NHC ligand design, enabling steric differentiation around the metal center.[10a] These ligand architectures balance steric bulk and accessible coordination sites, permitting precise control of catalytic reac-

[a]*Department of Chemistry and Pharmacy, Opole University, 48 Oleska Street, Opole 45-052, Poland. E-mail: ebisz@uni.opole.pl*
[b]*Department of Chemistry, Wroclaw University of Science and Technology, Norwida 4/6, Wroclaw 50-373, Poland*
[c]*Department of Chemistry, Wroclaw University, F. Joliot-Curie 14, Wroclaw 50-383, Poland*
[d]*Department of Chemistry, Rutgers University, 73 Warren Street, Newark, NJ 07102, USA. E-mail: michal.szostak@rutgers.edu*

Published on 06 2025. Downloaded on 06.01.2026 02:10:48.

tivity and selectivity. One of the most useful spatially-defined yet sterically-hindered N-heterocyclic carbenes is the unsymmetrical IPaul ligand introduced by Nelson and co-workers.[10a] The IPaul ligand features a pronounced steric differentiation—two quadrants providing substantial bulk and two remaining relatively open quadrants—and this ligand has demonstrated remarkable catalytic efficiency, including in copper-catalyzed hydrosilylation,[14,10a] Ni-catalyzed Suzuki–Miyaura coupling[15] and Kumada coupling.[16]

Considering the demonstrated benefits of NHC ligands featuring chelating heterocyclic donors and the advantages of the spatially defined steric architecture of IPaul, we envisioned integrating these two innovative strategies. Herein, we report the synthesis, application, and structural and electronic characterization of a novel class of 'bulky yet flexible' NHC ligands, which combine N,C chelating oxazole and thiazole wingtips with a spatially defined IPaul steric impact. The steric, electron-donating, and π-accepting characteristics, as well as coordination chemistry with Ag(I), Pd(II), Se and Rh(I), are reported. Furthermore, catalytic studies in cross-coupling and hydrosilylation catalyzed by Ag, Pd, and Rh complexes are established. Overall, the design of this class of hybrid ligands exploits robust metal stabilization coupled with enhanced catalytic activity *via* sterically controlled hemilabile coordination and is well-suited for diverse catalytic applications. We anticipate that the combination of steric flexibility with N,C-chelation in versatile N-heterocyclic carbenes will be of broad interest across organometallic, inorganic and catalytic chemistry (Fig. 1).

Results and discussion

Our study commenced with the synthesis of IPaul^{Oxa} and IPaul^{Thia} imidazolium precursors featuring an IPaul moiety and N-oxazole or N-thiazole wingtips (Scheme 1). This design has been selected on the basis of the utility and accessibility of benzoxazoles and benzothiazoles as among the most versatile N-heterocyclic motifs in organic synthesis.[17] Specifically, benzoxazoles and benzothiazoles provide flexible chelation

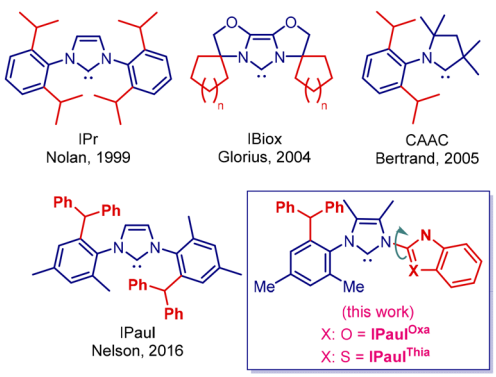

Fig. 1 State-of-the-art of sterically-demanding N-heterocyclic carbenes in inorganic and organometallic chemistry.

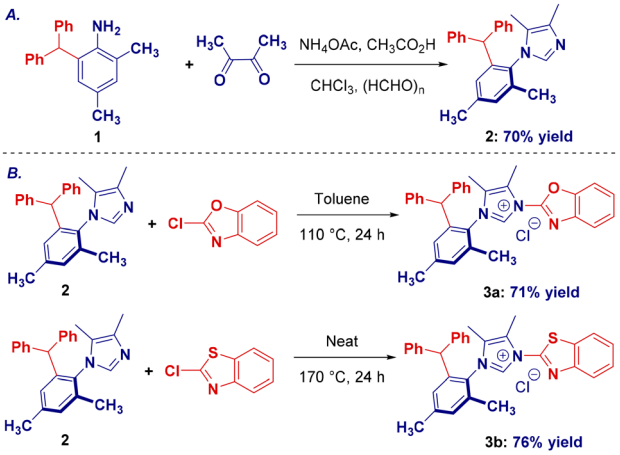

Scheme 1 Synthesis of imidazolium precursors. (A) Synthesis of 1-arylimidazole **2**; (B) synthesis of imidazolium salts **3a–3b**.

through their nitrogen and/or sulfur atoms, enabling tailored metal coordination environments with distinct steric and electronic properties.[13] Furthermore, many distinct synthetic routes to benzoxazoles and benzothiazoles are known, offering wide-ranging applications in coordination chemistry.[13] The developed synthesis follows a two-step modular approach involving (1) condensation between the corresponding aniline and diacetyl and (2) arylation with 2-halobenzazoles (Scheme 1A and B).

After optimization, we found that the desired condensation with benzoxazole proceeded in toluene under reflux conditions, while the reaction with benzothiazole occurred under additive-free conditions by heating a mixture of *N*-aryl imidazole and 2-chlorobenzothiazole. This approach is highly modular and should enable the synthesis of analogues using a condensation/S_NAr arylation sequence. It is worth noting that backbone 4,5-dimethyl substitution of the imidazole ring is preferred due to the higher stability of NHC salts and NHC–metal complexes.[18] The developed sequence is highly practical and permits the preparation of imidazolium precursors on a gram scale, without the need for chromatographic purification during the synthesis. Imidazolium salts **3a** and **3b** were obtained as bench-stable, crystalline solids, with melting points of 224–225 °C for **3a** and 258–259 °C for **3b**.

With the access to IPau^{Het} imidazolium precursors secured, we next evaluated the coordination chemistry of these spatially-defined, chelating azole-donor N-heterocyclic carbene ligands (Schemes 2–5). As shown in Scheme 2, we synthesized dimeric Ag(I)–NHC complexes **4a–4b** using imidazoliums **3a–3b**. Thus, [Ag(IPaul^{Oxa})(μ-Cl)]$_2$ (**4a**) and [Ag(IPaul^{Thia})(μ-Cl)]$_2$ (**4b**) were synthesized in 64–72% yields through the procedure reported by Gimeno and co-workers using $AgNO_3/K_2CO_3$ in CH_2Cl_2 at room temperature (Scheme 2).[19] The complexes were found to be stable in air and moisture.

Next, we also prepared chelating Pd(II)–NHC complexes, [Pd(IPaul^{Oxa})Cl$_2$] (**5a**) and [Pd(IPaul^{Thia})Cl$_2$] (**5b**), to evaluate the N,C coordination of these hemilabile *N*-azolyl-imidazol-2-

This journal is © The Royal Society of Chemistry 2025

Published on 06 2025. Downloaded on 06.01.2026 02:10:48.

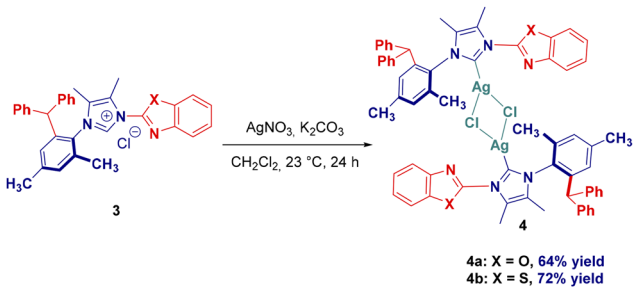

Scheme 2 Synthesis of Ag(I)–NHC complexes **4a–4b**.

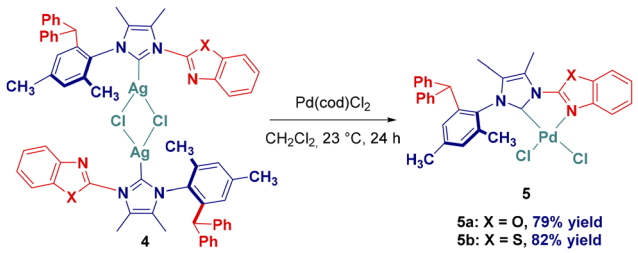

Scheme 3 Synthesis of Pd(II)–NHC complexes **5a–5b**.

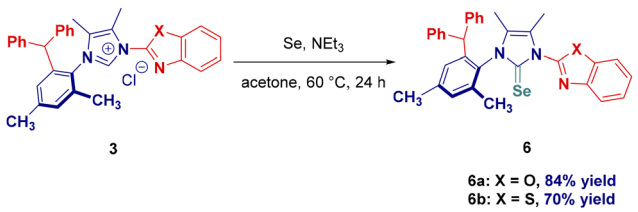

Scheme 4 Synthesis of Se–NHC complexes **6a–6b**.

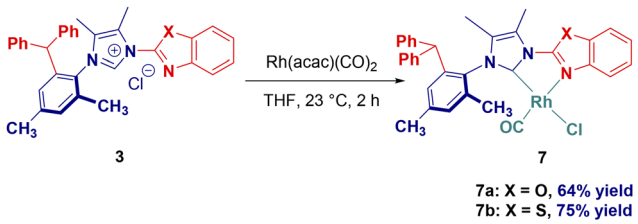

Scheme 5 Synthesis of Rh(I)–NHC complexes **7a–7b**.

ylidene ligands (Scheme 3). Thus, [Pd(IPaul^{Oxa})Cl$_2$] (**5a**) and [Pd(IPaul^{Thia})Cl$_2$] (**5b**) were synthesized by transmetallation of dimeric Ag(I) complexes **4a–4b** with [Pd(cod)Cl$_2$] at room temperature.[20] Pd(II)–NHC complexes **5a** and **5b** were obtained as air-stable solids in 79% and 82% yields, respectively.

To evaluate the electronic properties of this class of N,C-chelating ligands, we prepared selenourea adducts **6a** and **6b** (Scheme 4). π-Backbonding was assessed from the ^{77}Se NMR spectra of these selenoadducts using the standard procedure developed by Nolan *et al.*[21] In our experience, ^{77}Se measurements are strongly affected by the type of N-heterocyclic carbene system, as expected on the basis of the previous study.[21] The δ_{Se} value of 92 ppm for [Se(IPaul^{Oxa})] (**6a**) and 128 ppm for [Se(IPaul^{Thia})] (**6b**) can be compared with that of IPaul (δ_{Se} = 51 ppm for rotamer A and 64 ppm for rotamer B) and IPr* (δ_{Se} = 106 ppm).[22] In addition, **6a** and **6b** can be compared with their IPr* analogues: [Se(IPr*^{Oxa})] (δ_{Se} = 119 ppm)[13a] and [Se(IPr*^{Thia})] (δ_{Se} = 152 ppm).[23] It can therefore be concluded that both the increased N-steric substitution and N-heterocyclic substitution enhance the π-acceptor character of these ligands.

We also synthesized the chelating cationic [Rh(IPaul^{Oxa})(CO)Cl] (**7a**) and [Rh(IPr*^{Thia})(CO)Cl] (**7b**) complexes to further evaluate the electronic properties of this class of ligands. The Rh(I) complexes were prepared by the direct reaction of the imidazolium precursors **3a** or **3b** with [Rh(acac)(CO)$_2$] (Scheme 5). These Rh(I)–NHC **7a** and **7b** complexes are characterized by the CO stretching at 1988 and 1982 cm^{-1}, respectively. These values indicate an enhancement of π-backbonding of the ligands.[24]

Complexes **4a–4b** and **5b** were characterized by X-ray crystallographic analysis (Fig. 2). Despite many attempts we were unable to obtain X-ray quality crystals of **5a**; in this case, all assignments are based on analogy to **5b**. The silver complexes [Ag(IPaul^{Oxa})(μ-Cl)]$_2$ and [Ag(IPaul^{Thia})(μ-Cl)]$_2$ were found to be dimeric, while the palladium complex [Pd(IPaul^{Thia})Cl$_2$] was monomeric. Single-crystal diffraction of [Ag(IPaul^{Oxa})(μ-Cl)]$_2$ (Fig. 2I.A and B) shows that the complex crystallizes as a centrosymmetric chloride-bridged dimer in the monoclinic space group *I*2/*a*. The two Ag(I) centers are linked by a pair of bridging chlorides to yield an almost planar Ag$_2$Cl$_2$ four-membered ring (Cl1–Ag1–Cl1′ 93.88(3)°; Ag1–Cl1–Ag1′ 86.12(3)°). Each silver atom adopts a distorted T-shaped environment composed of the N-heterocyclic carbene carbon (C1), one terminal chloride and one bridging chloride (Ag1–C1(carbene) = 2.102(3) Å, Ag1–Cl1(terminal) = 2.3786(8) Å, Ag1–Cl1′(bridging) = 2.9283(8) Å, C1–Ag1–Cl1(quasi-linear) = 161.15(8)°, C1–Ag1–Cl1′ = 103.19(8)°, and Cl1–Ag1–Cl1′ 93.88(3)°). The benzoxazole ring remains essentially coplanar with the imidazolyl core (torsion C1–N1–C2–O1 ≈ 6°) and the oxygen atom is positioned away from the metal, mirroring the behavior observed previously in IPr*^{Oxa} complexes.[13a] The crystallographic metrics of [Ag(IPaul^{Thia})(μCl)]$_2$ (Fig. 2II.A and B) are closely comparable to those in the oxazole analogue; however, the Ag–Cl(bridge) distance is slightly shorter, indicating a marginally more compact Ag$_2$Cl$_2$ core (Ag1–C1(carbene) = 2.104(6) Å, Ag1–Cl1(terminal) = 2.387(2) Å, Ag1′–Cl1(bridging) = 2.8464(18) Å, C1–Ag1–Cl1 = 156.68(15)°, and C1–Ag1–Cl1′ = 107.89(15)°). The thiazolyl ring is essentially coplanar with the imidazol-2-ylidene backbone (C1(carbene)–N1–C2–S1 torsion ≈ 9°). The sulfur atom points toward the silver centre and forms a weak secondary contact (Ag···S ≈ 3.5 Å), indicating modest Ag···S interaction as also observed in related IPr*^{Thia} systems.[23]

The X-ray crystal structure analysis of [Pd(IPaul^{Thia})Cl$_2$] (Fig. 2III.B) revealed that the complex crystallizes as a monomeric species in the triclinic space group *P*$\bar{1}$. The palladium atom adopts the expected square-planar coordination defined

Published on 06 2025. Downloaded on 06.01.2026 02:10:48.

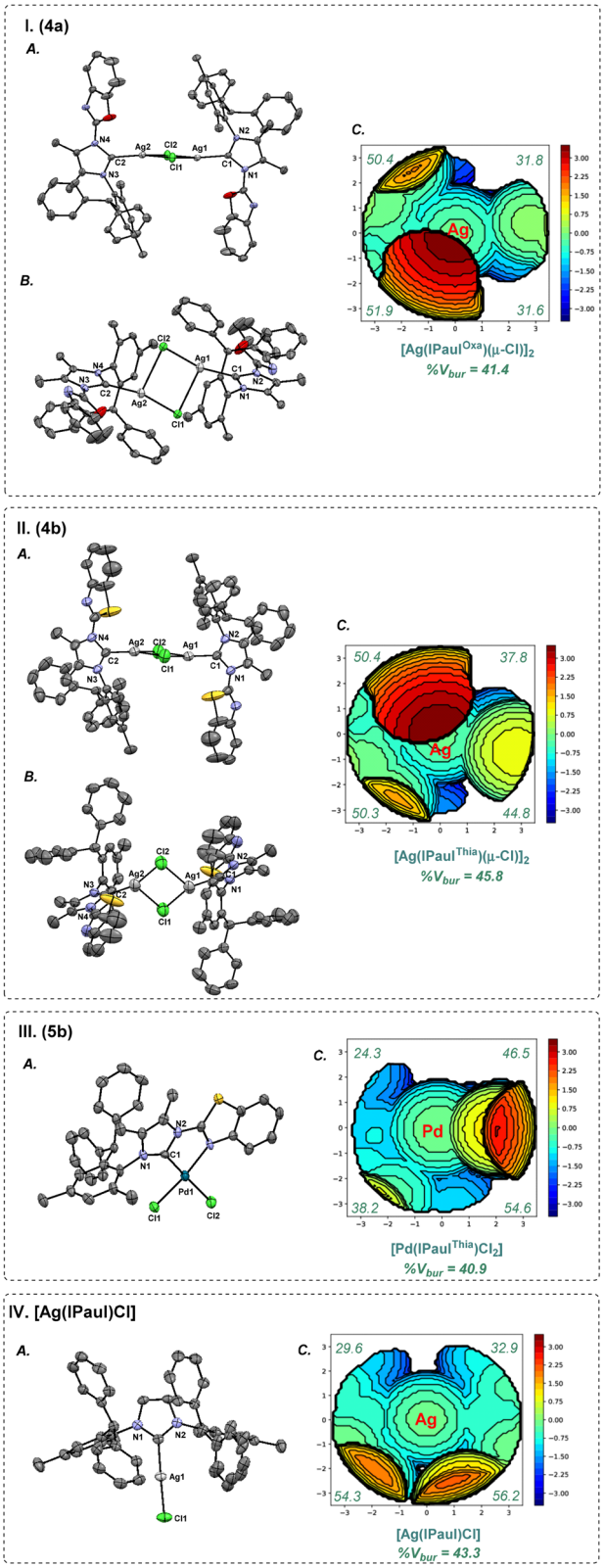

Fig. 2 X-ray crystal structures of complexes **4a** (I), **4b** (II), **5b** (III) and Ag(IPaul)Cl(IV).[10a] Two views of **4a** and **4b**: front (A); side (B). Hydrogen atoms have been omitted for clarity. Selected bond lengths [Å] and angles [°], see the SI. (C) Topographical steric map of complexes **4a**, **4b**, **5b** and Ag(IPaul)Cl showing $\%V_{bur}$ per quadrant. **4a**: CCDC 2452824, **4b**: CCDC 2452825 and **5b**: CCDC 2452826.

by the N-heterocyclic carbene carbon (C1), the thiazolyl nitrogen (N1), and two mutually trans chloride ligands (C1 (carbene)–Pd1 1.968(7) Å, N3(thiazolyl)–Pd1 2.092(5) Å, Pd1–Cl1 2.2655(18) Å, Pd1–Cl2 2.3492(18) Å, C1–Pd1–N3 bite angle 79.4(2)°, C1–Pd1–Cl2 175.38 (19)°, and N3–Pd1–Cl1 172.51 (15)°). Importantly, the thiazolyl ring is essentially coplanar with the imidazolyl core (torsion C1–N2–C3–N1 ≈ 1°), allowing efficient N,C-chelation. The benzhydryl IPaul wingtips adopt the characteristic *syn*-orientation. In this geometry, both trans axes are sterically-encumbered with the N–Pd–Cl axis being slightly more crowded than the C–Pd–Cl axis.

The geometry of complexes **4a–4b** was further analyzed using the method developed by Nolan, Cavallo and co-workers[25] to evaluate catalytic pockets (Fig. 2). The % buried volume ($\%V_{bur}$) of [Ag(IPaul^{Oxa})(μ-Cl)]$_2$ (**4a**) revealed a total buried volume of 41.4%, with the following quadrant distribution: SW, 51.9%; NW, 50.4%; NE, 31.8%; and SE, 31.6% for each quadrant (Fig. 2I.C; Ag2: ($\%V_{bur}$) of 41.4% with 50.4%, 51.9%, 31.6%, and 31.8% for each quadrant). The $\%V_{bur}$ value of the [Ag(IPaul^{Thia})(μ-Cl)]$_2$ (**4b**) complex is 45.8% with a quadrant distribution of SW, 50.3%; NW, 50.4%; NE, 37.8%; and SE, 44.8% (Fig. 2II.C; Ag2: ($\%V_{bur}$) of 45.8% with 49.3%, 40.3%, 54.8%, and 39.0% for each quadrant). It is worth noting that the classic IPaul ligand delivers IPr-class steric bulk,[26] but distributes it asymmetrically: the SW and SE quadrants form a rigid steric barrier (>50% coverage), with the quadrant distribution of NW, 29.6%, and NE, 32.9% (Fig. 2IV. C).[10a] It should be noted that the IPaul scaffold in **4a** and **4b** complexes also delivers IPaul-level bulk combined with pronounced quadrant asymmetry: a steric shielding in the western half and a tunable pocket to the east. Oxazole and thiazole wingtips offer a convenient handle for fine-tuning the pocket width, while retaining the hallmark bulky-yet-flexible character that underpins the catalytic success of the IPaul ligand class.

The % buried volume analysis of [Pd(IPaul^{Thia})Cl$_2$] (**5b**) shows a total $\%V_{bur}$ of 40.9% (SW 38.2%, NW 24.3%, NE 46.5%, and SE 54.6%). Compared with the Ag(I) [Ag(IPaul^{Thia})(μ-Cl)]$_2$ dimer (**4b**), the thiazole wingtip in **5b** rotates to lie almost coplanar with the square-planar Pd centre. This rotation transfers steric bulk from the western to the eastern hemisphere, narrowing the NW quadrant and enlarging the NE/SE quadrants, as clearly reflected in the quadrant distribution of the topographical steric map (Fig. 2III.C).

We briefly evaluated the catalytic activity of these spatially-defined N,C-chelating azolyl-donor ligands in Ag(I), Pd(0) and Rh(I) catalysis (Scheme 6). As shown, [Ag(IPaul^{Oxa})(μ-Cl)]$_2$ (**4a**) and [Ag(IPaul^{Thia})(μ-Cl)]$_2$ (**4b**) exhibit promising activity in Ag(I)-catalyzed A^3-coupling, which is slightly lower than that observed with [Ag(IPr)Cl] (98% yield)[27] but comparable to those observed with [Ag(IPr*)Cl] (80% yield) and [Ag(IPaul)Cl] (86% yield) (not shown). In contrast, in the alkynylation of isatins, complex **4a** demonstrated higher activity than [Ag(IPr)Cl] (93% yield),[28] [Ag(IPr*)Cl] (74% yield), and [Ag(IPaul)Cl] (66% yield) (not shown). The complexes [Pd(IPaul^{Oxa})Cl$_2$] (**5a**) and [Pd(IPaul^{Thia})Cl$_2$] (**5b**) performed well in the Heck coup-

This journal is © The Royal Society of Chemistry 2025

Published on 06 2025. Downloaded on 06.01.2026 02:10:48.

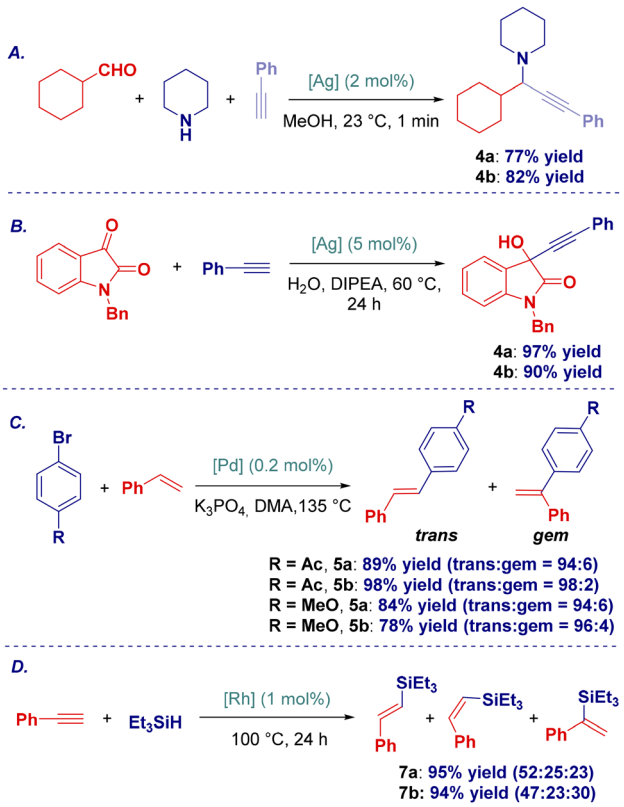

Scheme 6 Catalytic activity of [IPaul^{Het}–M] complexes: (A) A^3-coupling, (B) alkynylation of isatins, (C) Heck coupling, (D) hydrosilylation of terminal alkynes.

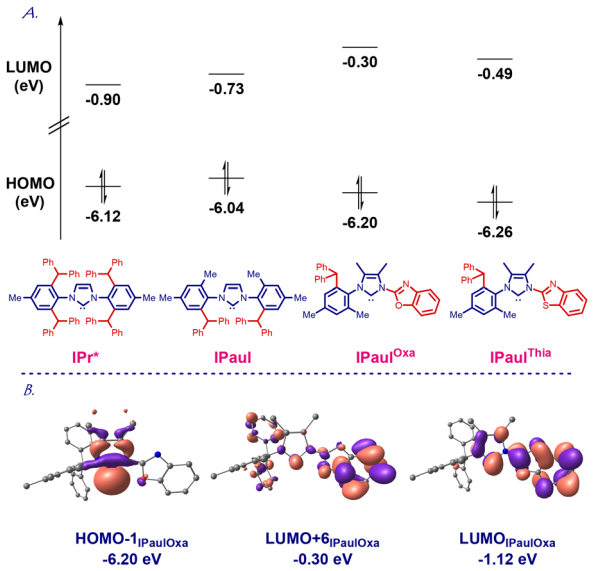

Fig. 3 (A) HOMO and LUMO energy levels (eV). (B) HOMO–1, LUMO+6 and LUMO (eV) of IPaul^{Oxa} calculated at B3LYP 6-311++g(d,p). See the SI.

ling, showing similar reactivity and selectivity to oxazole and thiazole analogues with IPr* and IPr*^{MeO} moieties.[13a,24] Finally, [Rh(IPaul^{Oxa})(CO)Cl] (**7a**) and [Rh(IPaul^{Thia})(CO)Cl] (**7b**) were found to efficiently catalyze hydrosilylation of terminal alkynes. Complexes **7a**–**7b** should be compared with Rh(I)–NHCs containing hemilabile N-donors, which typically exhibit higher *E*-selectivity.[29] These results indicate a high degree of generality of this class of ligands in valuable C–N, C–C and C–Si bond forming reactions. Our ongoing research focuses on the synthetic applications of this class of unsymmetrical ligands. The results will be reported in due course.

To gain insight into the electronic structure of these spatially-defined N,C-chelating IPaul^{Het} ligands, HOMO and LUMO energy levels were determined at the B3LYP 6-311++g(d,p) level (Fig. 3). It is now well established that the computed HOMO and LUMO provide the most accurate determination of the nucleophilicity and electrophilicity of N-heterocyclic carbene ligands. The σ-donor orbital of IPaul^{Oxa} (HOMO−1 due to required symmetry, −6.20 eV) can be compared with the sterically-hindered IPr* (−6.12 eV) and the classical IPr (−6.01 eV) as well as with the parent IPaul (−6.04 eV). The HOMO−1 of IPaul^{Thia} is in the same range (−6.36 eV). The π-accepting orbital of IPaul^{Oxa} (LUMO+6 due to required symmetry, −0.30 eV) and IPaul^{Thia} (LUMO+4 due to required symmetry, −0.49 eV) can be compared with the sterically-hindered IPr* (−0.90 eV), the classical IPr (−0.48 eV) and the parent IPaul (−0.73 eV). The LUMO of IPaul^{Oxa} (−1.12 eV) and the LUMO of IPaul^{Thia} (−1.25 eV) are located on the benzoxazole and benzothiazole rings, as expected. The π-donating orbital of IPaul^{Oxa} (HOMO, −6.15 eV) and the π-donating orbital of IPaul^{Thia} (HOMO, −6.07 eV) can be compared with those of the sterically-hindered IPr* (−6.28 eV) and the classical IPr (−6.55 eV) as well as with that of the parent IPaul (−6.29 eV). Overall, these results confirm IPaul^{Oxa} and IPaul^{Thia} as strongly σ-nucleophilic, spatially-distinct N-heterocyclic carbenes with electronic properties affected by the coordinating benzoxazole and benzothiazole rings. The combination of spatially-flexible IPaul substitution with coordinating N,C-heterocycles provides a sterically-unique chelating environment around the metal centers.

Conclusions

In summary, IPaul has emerged as a highly attractive spatially-defined N-heterocyclic carbene ligand that retains the properties of sterically-hindered IPr*, while providing a flexible environment featuring a pronounced steric differentiation. The utility of IPaul in an organometallic toolbox is reflected by its commercial availability. In this study, we reported a new class of IPaul-based ligands bearing benzoxazole and benzothiazole donor wingtips. These ligands retain the defining 'bulky yet flexible' profile of IPaul, while enabling precise control over the catalytic pocket geometry through N-heteroaryl wingtip substitution. We presented their coordination chemistry with Ag(I), Pd(II), Rh(I) and Se as well as catalytic studies in cross-coupling and hydrosilylation catalyzed by Ag, Pd, and Rh complexes. By combining the steric wingtip asymmetry of IPaul with the chelating flexibility of N-azole

Published on 06 2025. Downloaded on 06.01.2026 02:10:48.

donors, this ligand class provides stabilization of reactive metal centers and is well-suited for diverse catalytic applications. The combination of steric flexibility with N,C-chelation in versatile N-heterocyclic carbenes will be of broad interest across organometallic, inorganic and catalytic chemistry.

Experimental

General methods

All experiments involving metal complexes were performed using standard Schlenk techniques under nitrogen or argon unless stated otherwise. All solvents were of the highest commercial grade and used as received or after purification by distillation from sodium/benzophenone under nitrogen. All solvents were deoxygenated prior to use. All other chemicals were of the highest commercial grade and used as received. Compounds **1a**[10a] and **2a**[30] have been previously reported in the literature. Their spectroscopic properties matched literature data. ^{1}H NMR and ^{13}C NMR spectra were recorded using Bruker spectrometers at 400 (^{1}H NMR) and 100 MHz (^{13}C NMR). Infrared spectra were recorded using a Nicolet Nexus 2002 FTIR spectrometer. High-resolution mass spectroscopy (HRMS) and elemental analyses were performed using a 7T Bruker Daltonics FT-MS and a Vario EL II (CHNS) instrument, respectively.

Procedure for the synthesis of 2-(diphenylmethyl)-4,6-dimethylaniline (1a)

Aniline was synthesized according to a literature procedure.[10a] The product was obtained in 73% yield (22.00 g, 76.5 mmol) as a white solid. ^{1}H NMR (400 MHz, $CDCl_3$) δ 7.28 (dd, J = 7.9, 6.4 Hz, 4H), 7.22 (t, J = 6.2 Hz, 2H), 7.14–7.11 (m, 4H), 6.81 (s, 1H), 6.34 (d, J = 1.3 Hz, 1H), 5.47 (s, 1H), 3.33 (s, 2H), 2.12 (s, 3H), 2.11 (s, 3H). ^{13}C NMR (101 MHz, $CDCl_3$) δ 142.91, 139.99, 129.71, 129.66, 128.75, 128.66, 128.54, 127.02, 126.71, 122.74, 52.54, 20.85, 17.88.

Procedure for the synthesis of 1-(2-benzhydryl-4,6-dimethylphenyl)-4,5-dimethyl-1*H*-imidazole (2a)

N-Aryl imidazole was synthesized according to a modified literature procedure.[18b] To an aniline derivative (12 mmol) in dry $CHCl_3$ (20 mL), diacetyl (10 mmol), acetic acid (50 mmol), NH_4OAc (12 mmol), paraformaldehyde (10 mmol), and H_2O (0.5 mL) were added and the mixture was refluxed for 48 h. After removal of the solvent, the dark residue was dissolved in Et_2O and basified to pH 14 in an ice bath with aqueous 40% KOH solution. The resulting mixture was extracted with Et_2O, and the combined organic layers were washed with H_2O and dried over Na_2SO_4. Concentration and purification through silica gel column chromatography yielded the desired product. The product was obtained in 70% yield (3.50 g, 9.54 mmol) as a pale brown solid after purification by flash chromatography (hexane/AcOEt = 2/1). ^{1}H NMR (400 MHz, $CDCl_3$) δ 7.25–7.18 (m, 6H), 7.01 (s, 1H), 6.95 (d, J = 7.8 Hz, 4H), 6.92 (s, 1H), 6.80 (s, 1H), 5.09 (s, 1H), 2.29 (s, 3H), 2.20 (s, 3H), 1.89 (s, 3H), 1.59 (s, 3H). ^{13}C NMR (101 MHz, $CDCl_3$) δ 142.86, 142.65, 142.40, 138.83, 136.66, 135.01, 133.82, 132.43, 129.79, 129.55, 129.29, 128.87, 128.50, 128.31, 126.61, 126.56, 123.05, 51.45, 21.54, 17.61, 13.07, 8.09. HRMS (ESI/Q-TOF) m/z: $[M + H]^+$ calcd for $C_{26}H_{26}N_2$ 367.2095, found 367.2175.

Procedure for the synthesis of 1-(benzoxazol-2-yl)-3-IPaul imidazolium chloride (3a)

The product was synthesized according to a literature procedure.[13a] 1-Arylimidazole **2a** was added to a solution of 2-chlorobenzoxazole in toluene, and the mixture was heated at reflux overnight. During the course of the reaction, a white precipitate formed and the product was isolated by filtration. The solid was washed twice with Et_2O and dried *in vacuo*, affording the desired imidazolium salt.

New compound. The product was obtained in 71% yield (1.0 g, 1.92 mmol) as a white powder of mp 224–225 °C. ^{1}H NMR (400 MHz, $CDCl_3$) δ 11.23 (s, 1H), 7.80–7.77 (m, 1H), 7.73 (dd, J = 6.3, 2.6 Hz, 1H), 7.47–7.44 (m, 2H), 7.24 (d, J = 5.7 Hz, 7H), 7.18–7.15 (m, 1H), 7.12 (s, 1H), 6.99–6.96 (m, 2H), 6.70 (s, 1H), 5.43 (s, 1H), 2.66 (s, 3H), 2.29 (s, 3H), 2.15 (s, 3H), 1.64 (s, 3H). ^{13}C NMR (101 MHz, $CDCl_3$) δ 149.25, 148.77, 141.75, 141.14, 140.99, 140.57, 139.87, 138.58, 135.64, 130.98, 129.78, 129.50, 129.46, 128.82, 128.75, 128.28, 127.25, 127.01, 126.93, 126.02, 120.74, 111.94, 52.19, 21.64, 18.16, 11.01, 8.07. HRMS (ESI/Q-TOF) m/z (%) $[M]^+$ calcd for $C_{33}H_{30}N_3O^+$ 484.2388, found 484.2389.

Procedure for the synthesis of 1-(benzothiazol-2-yl)-3-IPaul imidazolium chloride (3b)

The product was synthesized according to a modified literature procedure.[13c] 1-Arylimidazole **2a** and 2-chlorobenzothiazole were stirred in a closed pressure tube for 20 h at 140 °C. The reaction mixture was then allowed to cool to room temperature and washed with diethyl ether until the supernatant became colorless. Product **3b** was then dried *in vacuo* to afford the desired imidazolium salt.

New compound. The product was obtained in 76% yield (0.35 g, 0.65 mmol) as a beige powder of mp 258–259 °C. ^{1}H NMR (400 MHz, $CDCl_3$) δ 11.18 (s, 1H), 8.05 (d, J = 8.1 Hz, 1H), 7.95 (d, J = 8.1 Hz, 1H), 7.59 (dd, J = 11.3, 4.2 Hz, 1H), 7.55–7.50 (m, 1H), 7.30–7.21 (m, 8H), 7.15 (td, J = 5.8, 3.2 Hz, 1H), 7.11 (s, 1H), 6.99 (d, J = 6.4 Hz, 2H), 5.51 (s, 1H), 2.54 (s, 3H), 2.28 (s, 3H), 2.17 (s, 3H), 1.66 (s, 3H). ^{13}C NMR (101 MHz, $CDCl_3$) δ 153.19, 149.70, 141.58, 141.31, 140.96, 140.93, 138.78, 135.79, 134.70, 130.98, 129.75, 129.58, 129.50, 129.01, 128.89, 128.75, 128.44, 127.71, 127.42, 127.16, 123.89, 122.47, 52.25, 21.64, 18.26, 10.96, 8.21. HRMS (ESI/Q-TOF) m/z (%) $[M]^+$ calcd for $C_{33}H_{30}N_3S^+$ 500.2160, found 500.2137.

General procedure for the synthesis of $[Ag(NHC)(\mu\text{-}Cl)]_2$ complexes

Ag(I)–NHC complexes were synthesized according to a modified literature procedure.[19] A mixture of an imidazolium salt (**3a** or **3b**) and $AgNO_3$ in dichloromethane was stirred for 2 min and then K_2CO_3 was added. After 24 h, the mixture was filtered through Celite and the solvent was removed *in vacuo*

 This journal is © The Royal Society of Chemistry 2025

Published on 06 2025. Downloaded on 06.01.2026 02:10:48.

until 2 mL remained (*ca.*). The product was precipitated with ether and washed to afford a white solid.

[Ag(IPaul^{Oxa})(μ-Cl)]$_2$ (4a)

New compound. The product was obtained in 64% yield (0.24 g, 0.19 mmol) as a white solid. Crystallization from CH_2Cl_2/Et_2O at RT yielded suitable crystals for X-ray diffraction studies. ^{1}H NMR (400 MHz, $CDCl_3$) δ 7.81–7.78 (m, 1H), 7.69–7.65 (m, 1H), 7.45–7.42 (m, 2H), 7.27–7.18 (m, 6H), 7.08 (d, J = 7.8 Hz, 3H), 6.97–6.94 (m, 2H), 6.76 (s, 1H), 5.37 (s, 1H), 2.48 (s, 3H), 2.32 (s, 3H), 1.97 (s, 3H), 1.38 (s, 3H). ^{13}C NMR (101 MHz, $CDCl_3$) δ 184.98, 182.26, 152.97, 149.37, 141.72, 141.13, 140.34, 140.22, 135.32, 133.47, 130.69, 130.12, 129.87, 129.68, 129.45, 128.99, 128.64, 127.10, 127.02, 126.43, 126.37, 126.29, 125.76, 120.57, 111.43, 51.95, 21.68, 18.04, 11.09, 8.46. Anal. calc. for $C_{66}H_{58}Ag_2Cl_2N_6O_2$ (1253.87): C, 63.22; H, 4.66; N, 6.70. Found: C, 63.60; H, 4.69; N, 6.67.

[Ag(IPaul^{Thia})(μ-Cl)]$_2$ (4b)

New compound. The product was obtained in 72% yield (0.26 g, 0.2 mmol) as a beige solid. Crystallization from CH_2Cl_2/Et_2O at RT yielded suitable crystals for X-ray diffraction studies. ^{1}H NMR (400 MHz, $CDCl_3$) δ 8.00 (dd, J = 8.1, 0.5 Hz, 1H), 7.88 (d, J = 7.5 Hz, 1H), 7.54 (dd, J = 7.6, 6.5 Hz, 1H), 7.48–7.45 (m, 1H), 7.32 (d, J = 7.5 Hz, 2H), 7.28–7.23 (m, 4H), 7.08 (s, 1H), 7.03 (d, J = 7.2 Hz, 2H), 6.97 (d, J = 6.6 Hz, 2H), 6.74 (s, 1H), 5.23 (s, 1H), 2.57 (s, 3H), 2.32 (s, 3H), 1.98 (s, 3H), 1.64 (s, 3H). ^{13}C NMR (101 MHz, $CDCl_3$) δ 184.18, 181.67, 158.87, 150.39, 141.65, 141.60, 141.44, 140.26, 135.53, 133.31, 133.11, 130.80, 129.76, 129.56, 129.37, 129.28, 128.64, 128.49, 128.42, 127.25, 127.12, 127.04, 126.44, 123.39, 122.15, 52.23, 21.67, 18.14, 11.68, 8.83. Anal. calc. for $C_{66}H_{58}Ag_2Cl_2N_6S_2$ (1285.99): C, 61.64; H, 4.55; N, 6.54. Found: C, 61.97; H, 4.57; N, 6.59.

General procedure for the synthesis of [Pd(NHC)Cl$_2$] complexes

Palladium complexes were synthesized according to a modified literature procedure.[20] [$PdCl_2$(1,5-COD)] was added to a solution of the Ag(I)–NHC complex (**4a** or **4b**) in CH_2Cl_2 with exclusion of light. The mixture became cloudy immediately. After one night at room temperature, the solution was filtered through Celite. The solvent was removed *in vacuo*.

[Pd(IPaul^{Oxa})Cl$_2$] (5a)

New compound. The product was obtained in 79% yield (0.15 g, 0.22 mmol) as a yellow solid. Crystallization from CH_2Cl_2/Hex at RT yielded suitable crystals for X-ray diffraction studies. ^{1}H NMR (400 MHz, $CDCl_3$) δ 8.70 (d, J = 7.4 Hz, 1H), 7.55 (d, J = 8.2 Hz, 1H), 7.50 (dd, J = 7.7, 6.9 Hz, 1H), 7.45–7.41 (m, 1H), 7.32 (d, J = 7.5 Hz, 4H), 7.27–7.18 (m, 4H), 7.11–7.02 (m, 1H) 6.96 (dd, J = 6.1, 3.3 Hz, 2H), 6.73 (s, 1H), 5.73 (s, 1H), 2.32 (s, 3H), 2.26 (s, 3H), 2.01 (s, 3H), 0.94 (s, 3H). ^{13}C NMR (101 MHz, $CDCl_3$) 149.31, 141.82, 141.45, 140.78, 140.05, 136.43, 134.61, 131.95, 131.40, 130.07, 130.00, 129.24, 128.51, 128.38, 126.99, 126.62, 126.45, 121.19, 111.41, 52.07, 21.77, 18.23, 9.34, 7.77. Anal. calcd for $C_{33}H_{29}Cl_2N_3OPd$ (660.94): C, 59.97; H, 4.42; N, 6.36. Found: C, 59.20; H, 4.39; N, 6.33.

[Pd(IPaul^{Thia})Cl$_2$] (5b)

New compound. The product was obtained in 82% yield (0.31 g, 0.45 mmol) as a yellow solid. Crystallization from CH_2Cl_2/Hex at RT yielded suitable crystals for X-ray diffraction studies. ^{1}H NMR (400 MHz, CD_2Cl_2) δ 9.81 (d, J = 8.2 Hz, 1H), 7.89–7.85 (m, 1H), 7.63–7.59 (m, 1H), 7.51 (dd, J = 8.2, 1.0 Hz, 1H), 7.23–7.18 (m, 4H), 7.14–7.10 (m, 4H), 7.00 (s, 1H), 6.87 (dd, J = 6.4, 3.1 Hz, 2H), 6.62 (s, 1H), 5.69 (s, 1H), 2.29 (s, 3H), 2.24 (s, 3H), 1.98 (s, 3H), 0.96 (s, 3H). ^{13}C NMR (101 MHz, CD_2Cl_2) δ 147.41, 144.36, 142.09, 141.27, 140.65, 139.71, 134.97, 132.57, 131.00, 129.76, 129.50, 128.87, 128.71, 128.34, 128.25, 126.88, 126.52, 124.42, 121.83, 52.01, 21.32, 17.83, 9.88, 7.74. Anal. calcd for $C_{33}H_{29}Cl_2N_3OPdS$ (677.00): C, 58.55; H, 4.32; N, 6.21. Found: C, 57.82; H, 4.29; N, 6.20.

General procedure for the synthesis of [Se(NHC)] complexes

The selenium complex was synthesized according to a modified literature procedure.[22] A 7 mL screwcap vial equipped with a septum cap and a stirring bar was charged with an imidazolium salt (**3a**) (0.16 g, 0.235 mmol, 1 equiv.), Se (0.02 g, 1.1 equiv.) and acetone (1 mL). The mixture was stirred at 40 °C for 15 min. NEt_3 (0.1 mL, 3 equiv.) was then added in one portion and the mixture was stirred overnight at 60 °C. Afterwards, the mixture was filtered through a plug of silica gel and washed with DCM (20 mL). All volatiles were then removed under vacuum. The product was obtained as a yellow microcrystalline material.

[Se(IPaul^{Oxa})] (6a)

New compound. The product was obtained in 84% yield (0.18 g, 0.32 mmol) as a yellow solid. Crystallization from CH_2Cl_2/Et_2O at −20 °C afforded suitable crystals for X-ray diffraction studies. ^{1}H NMR (400 MHz, $CDCl_3$) δ 7.90–7.86 (m, 1H), 7.70–7.66 (m, 1H), 7.45 (dd, J = 9.3, 3.5 Hz, 2H), 7.34 (d, J = 7.5 Hz, 2H), 7.22 (dd, J = 16.2, 9.2 Hz, 6H), 7.11 (d, J = 7.1 Hz, 2H), 7.06 (s, 1H), 6.77 (s, 1H), 5.67 (s, 1H), 2.29 (s, 3H), 2.04 (s, 3H), 2.01 (s, 3H), 0.93 (s, 3H). ^{13}C NMR (101 MHz, $CDCl_3$) δ 159.50, 151.35, 150.62, 143.39, 142.80, 140.99, 140.59, 139.68, 135.89, 131.93, 130.28, 130.11, 129.63, 129.57, 128.46, 128.13, 126.84, 126.57, 126.45, 126.39, 125.28, 123.86, 121.07, 111.53, 51.85, 21.69, 18.11, 9.56, 8.34. Anal. calc. for $C_{33}H_{29}N_3OSe$ (562.58): C, 70.46; H, 5.20; N, 7.47. Found: C, 70.14; H, 5.12; N, 7.40, ^{77}Se NMR (114 MHz, $CDCl_3$) δ 92.07.

[Se(IPaul^{Thia})] (6b)

New compound. The product was obtained in 70% yield (0.15 g, 0.26 mmol) as a yellow solid. Crystallization from CH_2Cl_2/Et_2O at −20 °C yielded suitable crystals for X-ray diffraction studies. ^{1}H NMR (400 MHz, $CDCl_3$) δ 8.03 (dd, J = 8.0, 0.5 Hz, 1H), 7.91 (dd, J = 7.9, 0.7 Hz, 1H), 7.54–7.50 (m, 1H), 7.47–7.43 (m, 1H), 7.33 (d, J = 7.5 Hz, 2H), 7.26–7.21 (m, 5H), 7.18 (d, J = 7.2 Hz, 1H), 7.07–7.04 (m, 3H), 6.78 (s, 1H), 5.58 (s, 1H), 2.30 (s, 6H), 2.01 (s, 3H), 0.97 (d, J = 0.7 Hz, 3H). ^{13}C NMR

Published on 06 2025. Downloaded on 06.01.2026 02:10:48.

(101 MHz, $CDCl_3$) δ 158.32, 157.09, 148.89, 143.34, 142.90, 140.99, 139.61, 135.97, 134.67, 132.41, 130.31, 130.13, 129.64, 128.49, 128.21, 126.85, 126.71, 126.45, 126.36, 125.92, 124.93, 123.25, 121.72, 51.93, 21.74, 18.18, 11.94, 8.42. Anal. calc. for $C_{33}H_{29}N_3SSe$ (578.64): C, 68.50; H, 5.05; N, 7.26. Found: C, 68.19; H, 5.00; N, 7.20, ^{77}Se NMR (114 MHz, $CDCl_3$) δ 127.61.

General procedure for the synthesis of [Rh(NHC)(CO)Cl] complexes

The rhodium complex was synthesized according to a modified literature procedure.[13] Solid $Rh(acac)(CO)_2$ (0.05 g, 0.194 mmol) and an imidazolium salt (**3a**) (0.05 g, 0.194 mmol) were weighed in a Schlenk tube in a glovebox. THF (10 mL) was then added, and the colour of the solution immediately turned yellow. After stirring for 2 h at room temperature, the solvent was removed *in vacuo*, and the crude product was washed twice with Et_2O, affording the rhodium complex as a yellow solid.

[Rh(IPaul^{Oxa})(CO)Cl] (7a)

New compound. The product was obtained in 64% yield (0.15 g, 0.23 mmol) as an orange solid. Crystallization from CH_2Cl_2/Et_2O at RT yielded suitable crystals for X-ray diffraction studies. ^{1}H NMR (400 MHz, $CDCl_3$) δ 8.69 (d, J = 7.8 Hz, 1H), 7.55 (d, J = 8.1 Hz, 1H), 7.40 (d, J = 7.6 Hz, 1H), 7.35 (t, J = 7.3 Hz, 1H), 7.27–7.23 (m, 4H), 7.20–7.16 (m, 4H), 7.02 (s, 1H), 6.96–6.93 (m, 2H), 6.76 (s, 1H), 5.73 (s, 1H), 2.32 (s, 3H), 2.26 (s, 3H), 2.01 (s, 3H), 0.94 (s, 3H). ^{13}C NMR (101 MHz, $CDCl_3$) δ 188.36, 187.55, 182.95, 182.36, 158.44, 149.69, 142.13, 142.04, 141.17, 140.59, 137.85, 135.86, 132.53, 130.28, 129.96, 129.72, 129.65, 128.55, 128.47, 127.13, 126.98, 126.72, 125.27, 121.01, 120.46, 110.76, 51.78, 21.74, 18.02, 9.54, 7.96. FT-IR (KBr): 1988 cm^{-1} ($\nu_{(C=O)}$), 1625 cm^{-1} ($\nu_{(C=N)}$). Anal. calc. for $C_{34}H_{29}ClN_3O_2Rh$ (649.98): C, 62.23; H, 4.50; N, 6.46. Found: C, 62.82; H, 4.50; N, 6.39.

[Rh(IPaul^{Thia})(CO)Cl] (7b)

New compound. The product was obtained in 75% yield (0.14 g, 0.21 mmol) as an orange solid. Crystallization from CH_2Cl_2/Et_2O at RT yielded suitable crystals for X-ray diffraction studies. ^{1}H NMR (400 MHz, $CDCl_3$) δ 9.75 (d, J = 8.5 Hz, 1H), 7.80 (d, J = 7.9 Hz, 1H), 7.59 (t, J = 7.1 Hz, 1H), 7.45–7.40 (m, 1H), 7.31–7.26 (m, 4H), 7.19 (s, 4H), 7.05 (s, 1H), 6.97 (s, 2H), 6.79 (s, 1H), 5.82 (s, 1H), 2.32 (d, J = 15.8 Hz, 6H), 2.06 (s, 3H), 0.99 (s, 3H). ^{13}C NMR (101 MHz, $CDCl_3$) δ 188.02, 187.21, 183.90, 183.31, 161.65, 148.95, 142.27, 142.14, 141.29, 140.53, 136.01, 133.07, 130.29, 129.99, 129.75, 129.70, 129.32, 129.17, 128.56, 128.41, 126.90, 126.69, 125.96, 124.61, 121.28, 119.85, 51.85, 21.76, 18.09, 10.31, 8.28. FT-IR (KBr): 1982 cm^{-1} ($\nu_{(C=O)}$), 1666 cm^{-1} ($\nu_{(C=N)}$). Anal. calc. for $C_{34}H_{29}ClN_3ORhS$ (666.04): C, 61.31; H, 5.32; N, 6.31. Found: C, 61.75; H, 5.30; N, 6.34.

General procedure for the three-component coupling reaction

A previously reported procedure was followed.[27,31] The reaction mixture was prepared according to the procedure using catalyst **4a** or **4b** (2 mol%), aldehyde (0.5 mmol), amine (0.55 mmol), alkyne (0.55 mmol) and MeOH (0.25 mL) and stirred at room temperature for 1 hour. After the desired time, the conversion was determined by ^{1}H NMR or GC analysis. The mixture was diluted with Et_2O and filtered over a pad of silica.

1-(1-Cyclohexyl-3-phenyl-2-propynyl)piperidine

The product was obtained in 82% yield (115.38 mg, 0.5 mmol) as a yellow liquid after purification by flash chromatography (petroleum ether/AcOEt = 10/1).

^{1}H NMR (400 MHz, CDCl3) δ 7.47–7.40 (m, 2H), 7.31–7.24 (m, 3H), 3.11 (d, J = 9.9 Hz, 1H), 2.63 (dd, J = 12.5, 5.5 Hz, 2H), 2.40 (d, J = 6.5 Hz, 2H), 2.08 (dd, J = 28.6, 13.7 Hz, 2H), 1.77 (d, J = 12.8 Hz, 2H), 1.60 (dd, J = 16.1, 4.8 Hz, 6H), 1.48–1.40 (m, 2H), 1.22 (dd, J = 20.7, 11.2 Hz, 3H), 1.07–0.90 (m, 2H). ^{13}C NMR (101 MHz, $CDCl_3$) δ ^{13}C NMR (101 MHz, $CDCl_3$) δ 131.92, 128.39, 127.81, 124.00, 87.99, 86.32, 64.59, 50.94, 39.79, 31.55, 30.64, 27.02, 26.51, 26.32, 24.94.

General procedure for alkynylation

A previously reported procedure was followed.[28] The reaction mixture was prepared according to the procedure using *N*-benzylisatin (0.5 mmol) and catalyst **4a** or **4b** (5 mol%) in water (2 ml), followed by the addition of phenylacetylene (1.0 mmol) and DIPEA (10 mol%). The reaction mixture was stirred for 24 hours at 60 °C and extracted with DCM (2 × 15 mL). After the desired time, the conversion was determined by ^{1}H NMR or GC analysis. The mixture was diluted with DCM and filtered over a pad of silica.

1-Benzyl-3-hydroxy-3-(phenylethynyl)indolin-2-one

The product was obtained in 97% yield (82 mg, 0.25 mmol) as a yellow liquid after purification by flash chromatography (petroleum ether/AcOEt = 4/1). ^{1}H NMR (400 MHz, $CDCl_3$) δ 7.64 (d, J = 8.1 Hz, 1H), 7.47 (d, J = 9.6 Hz, 2H), 7.34–7.24 (m, 9H), 7.14 (t, J = 8.0 Hz, 1H), 6.74 (d, J = 7.8 Hz, 1H), 4.95 (s, 2H), 3.89 (s, 1H). ^{13}C NMR (101 MHz, CDCl3) δ 174.40, 142.33, 135.15, 132.26, 130.63, 129.25, 129.11, 128.36, 127.62, 127.34, 124.07, 123.41, 121.73, 110.14, 86.79, 85.57, 69.81, 44.24.

General procedure for the Heck cross-coupling reaction

A previously reported procedure was followed.[21] According to the procedure, catalyst **5a** or **5b** (0.2 mol%), base (1.50 mmol), and Bu_4NBr (0.2 mmol) were placed in a Schlenk tube containing a small stirring bar. The Schlenk tube was subjected to evacuation/backfilling cycles with argon, and then styrene (2.0 mmol), di(ethylene glycol) dibutyl ether (0.50 mmol), DMA (2.5 mL), and the haloarene (1.0 mmol) were added. The mixture was then heated at 135 °C for 2–24 h. After the desired time, the conversion was determined by ^{1}H NMR or GC analysis. The mixture was diluted with Et_2O and filtered over a pad of silica.

E-1-(4-Styrylphenyl)ethenone

The product was obtained in 98% yield (108.92 mg, 0.5 mmol) as a yellow liquid after purification by flash chromatography (hexane/AcOEt = 10/1). ^{1}H NMR (400 MHz, CDCl3) δ 7.93 (d,

 This journal is © The Royal Society of Chemistry 2025

Published on 06 2025. Downloaded on 06.01.2026 02:10:48.

J = 8.4 Hz, 2H), 7.58–7.56 (m, 2H), 7.53–7.51 (m, 2H), 7.38–7.34 (m, 2H), 7.30–7.26 (m, 1H), 7.21 (d, J = 16.4 Hz, 1H), 7.11 (d, J = 16.4 Hz, 1H), 2.57 (s, 3H). ^{13}C NMR (101 MHz, CDCl3) δ 197.70, 142.17, 136.85, 136.09, 131.62, 129.06, 128.98, 128.50, 127.60, 126.99, 126.67, 26.80.

(*E*)-1-Methoxy-4-styrylbenzene

The product was obtained in 84% yield (88.32 mg, 0.5 mmol) as a yellow liquid after purification by flash chromatography (hexane/AcOEt = 10/1). ^{1}H NMR (400 MHz, CDCl3) δ 7.52–7.45 (m, 9H), 7.35 (dd, J = 10.8, 4.5 Hz, 4H), 7.27–7.23 (m, 3H), 7.03 (dd, J = 38.2, 16.3 Hz, 5H), 6.93–6.89 (m, 4H), 3.84 (s, 6H). ^{13}C NMR (101 MHz, CDCl3) δ 159.50, 137.84, 130.34, 128.86, 128.41, 127.93, 127.43, 126.81, 126.46, 114.33, 55.55.

General procedure for the hydrosilylation reaction

A previously reported procedure was followed.[13] According to the procedure, in a Schlenk tube, a solution of complex **7a** (0.005 mmol) in dry toluene (1.5 mL) was prepared, and phenylacetylene (0.5 mmol), triethylsilane (0.55 mmol), and *n*-dodecane (100 μL) were added in quick succession *via* a syringe. The bright yellow reaction mixture was stirred at 100 °C for 24 h. The crude mixture was filtered through alumina and analyzed by GC-MS. The solvent was evaporated and the products were purified by flash chromatography through a short plug of silica and analyzed by ^{1}H NMR spectroscopy. The three reaction products were determined on the basis of the olefinic coupling constants in the ^{1}H NMR (400 MHz, $CDCl_3$) spectra: (**7a**) β-(*Z*)-isomer: 7.44 (d, J = 9.2 Hz), 5.76 (d, J = 15.2 Hz); β-(*E*)-isomer: 6.89 (d, J = 19.4 Hz), 6.43 (d, J = 19.3 Hz); and α-isomer: ^{1}H NMR 5.87 (d, J = 3.1 Hz), 5.57 (d, J = 3.1 Hz). ^{1}H NMR (400 MHz, $CDCl_3$) spectra: (**7b**) β-(*Z*)-isomer: 7.44 (d, J = 8.3 Hz), 5.76 (d, J = 15.2 Hz); β-(*E*)-isomer: 6.84 (d, J = 19.2 Hz), 6.43 (d, J = 19.2 Hz); and α-isomer: ^{1}H NMR 5.87 (d, J = 3.1 Hz), 5.57 (d, J = 3.1 Hz).

Conflicts of interest

There are no conflicts to declare.

Data availability

The authors confirm that the data supporting this article have been included as part of the SI: experimental details and computational data. See DOI: **https://doi.org/10.1039/d5dt01576f**.

Additional raw data are available from the corresponding author upon reasonable request.

CCDC 2452824–2452826 contain the supplementary crystallographic data for this paper.[32a–32c]

Acknowledgements

We gratefully acknowledge Narodowe Centrum Nauki (grant no. 2019/35/D/ST4/00806), Rutgers University and the NIH (R35GM133326) for generous financial support. We thank the Wroclaw Center for Networking and Supercomputing (grant number WCSS159).

References

1 (*a*) D. Bourissou, O. Guerret, F. P. Gabbaï and G. Bertrand, *Chem. Rev.*, 2000, **100**, 39–92; (*b*) For the original study by Arduengo, see: A. J. Arduengo III, R. L. Harlow and M. Kline, *J. Am. Chem. Soc.*, 1991, **113**, 361–363; (*c*) A. J. Arduengo III, *Acc. Chem. Res.*, 1999, **32**, 913–921.

2 (*a*) M. N. Hopkinson, C. Richter, M. Schedler and F. Glorius, *Nature*, 2014, **510**, 485–496; (*b*) S. P. Nolan, *N-Heterocyclic Carbenes*, Wiley, 2014; (*c*) S. Diez-Gonzalez, *N-Heterocyclic Carbenes: From Laboratory Curiosities to Efficient Synthetic Tools*, *RSC*, 2016; (*d*) H. V. Huynh, *The Organometallic Chemistry of N-Heterocyclic Carbenes*, Wiley, 2017; (*e*) C. S. J. Cazin, *N-Heterocyclic Carbenes in Transition Metal Catalysis*, Springer, 2011; (*f*) E. A. B. Kantchev, C. J. O. O'Brien and M. G. Organ, *Angew. Chem., Int. Ed.*, 2007, **46**, 2768–2813; (*g*) W. A. Hermann, *Angew. Chem., Int. Ed.*, 2002, **41**, 1290–1309; (*h*) E. Peris, *Chem. Rev.*, 2018, **118**, 9988–10031; (*i*) G. Sipos and R. Dorta, *Coord. Chem. Rev.*, 2018, **375**, 13–68; (*j*) M. Iglesias and L. A. Oro, *Chem. Soc. Rev.*, 2018, **47**, 2772–2808; (*k*) A. A. Danopoulos, T. Simler and P. Braunstein, *Chem. Rev.*, 2019, **119**, 3730–3961; (*l*) Q. Zhao, G. Meng, S. P. Nolan and M. Szostak, *Chem. Rev.*, 2020, **120**, 1981–2048; (*m*) C. Chen, F. S. Liu and M. Szostak, *Chem. – Eur. J.*, 2021, **27**, 4478–4499; (*n*) R. Jazzar, M. Soleilhavoup and G. Bertrand, *Chem. Rev.*, 2020, **120**, 4141–4168; (*o*) J. Morvan, M. Mauduit, G. Bertrand and R. Jazzar, *ACS Catal.*, 2021, **11**, 1714–1748; (*p*) P. Gao and M. Szostak, *Coord. Chem. Rev.*, 2023, **485**, 215110.

3 (*a*) H. Clavier and S. P. Nolan, *Chem. Commun.*, 2010, **46**, 841–861; (*b*) A. Gomez-Suarez, D. J. Nelson and S. P. Nolan, *Chem. Commun.*, 2017, **53**, 2650–2660; (*c*) H. V. Huynh, *Chem. Rev.*, 2018, **118**, 9457–9492.

4 (*a*) M. Yus, C. Najcra, F. Foubelo and J. M. Sansano, *Chem. Rev.*, 2023, **123**, 11817–11893; (*b*) A. John and P. Ghosh, *Dalton Trans.*, 2010, **39**, 7183–7206; (*c*) S. Diez-Gonzalez and S. P. Nolan, *Coord. Chem. Rev.*, 2007, **251**, 874–883; (*d*) T. Dröge and F. Glorius, *Angew. Chem., Int. Ed.*, 2010, **49**, 6940–6952.

5 M. Koy, P. Bellotti, M. Das and F. Glorius, *Nat. Catal.*, 2021, **4**, 352–363.

6 (*a*) K. M. Lee, C. K. Lee and I. J. B. Lin, *Angew. Chem., Int. Ed. Engl.*, 1997, **36**, 1850–1852; (*b*) A. J. Boydston, K. A. Williams and C. W. Bielawski, *J. Am. Chem. Soc.*, 2005, **127**, 12496–12497; (*c*) J. L. Hickey, R. A. Ruhayel, P. J. Barnard, M. V. Baker, S. J. Berners-Price and A. Filipovska, *J. Am. Chem. Soc.*, 2008, **130**, 12570–12571; (*d*) K. M. Hindi, M. J. Panzner, C. A. Tessier, C. L. Cannon and W. J. Youngs, *Chem. Rev.*, 2009, **109**, 3859–3884; (*e*) L. Mercs and M. Albrecht, *Chem. Soc. Rev.*, 2010, **39**,

Published on 06 2025. Downloaded on 06.01.2026 02:10:48.

1903–1912; (*f*) K. Oisaki, Q. Li, H. Furukawa, A. U. Czaja and O. M. A. Yaghi, *J. Am. Chem. Soc.*, 2010, **132**, 9262–9264; (*g*) K. V. S. Ranganath, J. Kloesges, A. H. Schafer and F. Glorius, *Angew. Chem., Int. Ed.*, 2010, **49**, 7786–7789; (*h*) P. Lara, O. Rivada-Wheelaghan, S. Conejero, R. Poteau, K. Phillippot and B. Chaudret, *Angew. Chem., Int. Ed.*, 2011, **50**, 12080–12084; (*i*) A. V. Zhukhovitskiy, M. G. Mavros, T. V. Voorhis and J. A. Johnson, *J. Am. Chem. Soc.*, 2013, **135**, 7418–7421; (*j*) R. Visbal and M. C. Gimeno, *Chem. Soc. Rev.*, 2014, **43**, 3551–3574.

7 (*a*) A. Chartoire, M. Lesieur, L. Falivene, A. M. Z. Slawin, L. Cavallo, C. S. J. Cazin and S. P. Nolan, *Chem. – Eur. J.*, 2012, **18**, 4517–4521; (*b*) H. Lebel, M. K. Janes, A. B. Charette and S. P. Nolan, *J. Am. Chem. Soc.*, 2004, **126**, 5046–5047; (*c*) S. P. Nolan, *Acc. Chem. Res.*, 2011, **44**, 91–100.

8 (*a*) M. N. Hopkinson, C. Richter, M. Schedler and F. Glorius, *Nature*, 2014, **510**, 485–496; (*b*) M. Koy, P. Bellotti, M. Das and F. Glorius, *Nat. Catal.*, 2021, **4**, 352–363; (*c*) G. Altenhoff, R. Goddard, C. W. Lehmann and F. Glorius, *Angew. Chem., Int. Ed.*, 2003, **42**, 3690–3693; (*d*) G. Altenhoff, R. Goddard, C. W. Lehmann and F. Glorius, *J. Am. Chem. Soc.*, 2004, **126**, 15195–15201; (*e*) S. Würtz, C. Lohre, R. Fröhlich, K. Bergander and F. Glorius, *J. Am. Chem. Soc.*, 2009, **131**, 8344–8345.

9 (*a*) D. Martin, N. Lassauque, B. Donnadieu and G. Bertrand, *Angew. Chem., Int. Ed.*, 2012, **51**, 6172–6175; (*b*) D. Bourissou, O. Guerret, F. P. Gabbaï and G. Bertrand, *Chem. Rev.*, 2000, **100**, 39–92; (*c*) V. Lavallo, Y. Canac, C. Präsang, B. Donnadieu and G. Bertrand, *Angew. Chem.*, 2005, **117**, 5851–5855.

10 (*a*) P. Shaw, A. R. Kennedy and D. J. Nelson, *Dalton Trans.*, 2016, **45**, 11772–11780; (*b*) D. J. Nelson and S. P. Nolan, *Chem. Soc. Rev.*, 2013, **42**, 6723–6753.

11 (*a*) H. Valdés, D. Canseco-González, J. M. Germán-Acacio and D. Morales-Morales, *J. Organomet. Chem.*, 2018, **867**, 51–54; (*b*) F. Zhang, X. Lan, C. Xu, H. Yao, T. Li and F. Liu, *Org. Chem. Front.*, 2019, **6**, 3292–3299.

12 C. S. Slone, D. A. Weinberger and C. A. Mirkin, The Transition Metal Coordination Chemistry of Hemilabile Ligands, in *Progress in Inorganic Chemistry*, Wiley, 1999.

13 (*a*) P. Podchorodecka, B. Dziuk, R. Szostak, M. Szostak and E. Bisz, *Dalton Trans.*, 2023, **52**, 13608–13617; (*b*) M. Poyatos, A. Maisse-Francois, S. Bellemin-Laponnaz and L. H. Gade, *Organometallics*, 2006, **25**, 2634–2641; (*c*) D. Meyer, M. A. Taige, A. Zeller, K. Hohlfeld, S. Ahrens and T. Strassner, *Organometallics*, 2009, **28**, 2142–2149.

14 J. D. Egbert, C. S. J. Cazin and S. P. Nolan, *Catal. Sci. Technol.*, 2013, **3**, 912–926.

15 V. Ritleng, A. M. Oertel and M. J. Chetcuti, *Dalton Trans.*, 2010, **39**, 8153–8160.

16 M. Kardela, K. Halikowska-Tarasek, M. Szostak and E. Bisz, *Catal. Sci. Technol.*, 2022, **12**, 7275–7280.

17 (*a*) M. T. Chhabria, S. Patel, P. Modi and P. S. Brahmkshatriya, *Curr. Top. Med. Chem.*, 2016, **16**, 2841–2862; (*b*) S. H. Ali and A. R. Sayed, *Synth. Commun.*, 2020, **51**, 670–700; (*c*) A. Dondoni, *Org. Biomol. Chem.*, 2010, **15**, 3366–3385.

18 (*a*) M. Szostak, Q. Zhao and M. Rahman, US202163154948, 2021; (*b*) M. Kuriyama, N. Hamaguchi, G. Yano, K. Tsukuda, K. Sato and O. Onomura, *J. Org. Chem.*, 2016, **81**, 8934–8946.

19 R. Visbal, A. Laguna and M. C. Gimeno, *Chem. Commun.*, 2013, **49**, 5642–5644.

20 V. Cesar, S. Bellemin-Laponnaz and L. H. Gade, *Organometallics*, 2002, **21**, 5204–5208.

21 (*a*) S. V. C. Vummaleti, D. J. Nelson, A. Poater, A. Gomez-Suarez, D. B. Cordes, A. M. Z. Slawin, S. P. Nolan and L. Cavallo, *Chem. Sci.*, 2015, **6**, 1895–1904; (*b*) A. Liske, K. Verlinden, H. Buhl, K. Schaper and C. Ganter, *Organometallics*, 2013, **32**, 5269–5272; (*c*) G. P. Junor, J. Lorkowski, C. M. Weinstein, R. Jazzar, C. Pietraszuk and G. Bertrand, *Angew. Chem., Int. Ed.*, 2020, **59**, 22028–22033.

22 F. Nahra, K. Van Hecke, A. R. Kennedy and D. J. Nelson, *Dalton Trans.*, 2018, **47**, 10671–10684.

23 P. Podchorodecka, B. Dziuk, R. Szostak, R. Junga, M. Szostak and E. Bisz, *Dalton Trans.*, 2024, **53**, 14975–14985.

24 K. Azouzi, C. Duhayon, I. Benaissa, N. Lugan, Y. Canac, S. Bastin and V. Cesar, *Orgnaometallics*, 2018, **37**, 4726–4735.

25 L. Falivene, Z. Cao, A. Petta, L. Serra, A. Poater, R. Oliva, V. Scarano and L. Cavallo, *Nat. Chem.*, 2019, **11**, 872–879.

26 P. De Fremont, N. M. Scott, E. D. Stevens, T. Ramnial, O. C. Lightbody, C. L. B. Macdonald, J. A. C. Clyburne, C. D. Abernethy and S. P. Nolan, *Organometallics*, 2005, **24**, 6301–6309.

27 M. T. Chen, B. Landers and O. Navarro, *Org. Biomol. Chem.*, 2012, **10**, 2206–2208.

28 X. P. Fu, L. Liu, D. Wang, Y. L. Chen and C. J. Li, *Green Chem.*, 2011, **13**, 549–553.

29 J. P. Morales-Ceron, P. Lara, J. Lopez-Serrano, L. L. Santos, V. Salazar, E. Alvarez and A. Suarez, *Organometallics*, 2017, **36**, 2460–2469.

30 K. Halikowska-Tarasek, W. Ochędzan-Siodłak, B. Dziuk, R. Szostak, M. Szostak and E. Bisz, *Inorg. Chem.*, 2025, **64**, 7851–7857.

31 (*a*) M. T. Chen, B. Landers and O. Navarro, *Org. Biomol. Chem.*, 2012, **10**, 2206–2208; (*b*) Z. Wang, N. V. Tzouras, S. P. Nolan and X. Bi, *Trends Chem.*, 2021, **3**, 674–685; (*c*) S. Yang, T. Zhou, X. Yu and M. Szostak, *Molecules*, 2023, **22**, 1672.

32 (*a*) P. Podchorodecka, B. Dziuk, R. Szostak, M. Szostak and E. Bisz, CCDC 2452824: Experimental Crystal Structure Determination, 2025, DOI: **10.5517/ccdc.csd.cc2nbccr**; (*b*) P. Podchorodecka, B. Dziuk, R. Szostak, M. Szostak and E. Bisz, CCDC 2452825: Experimental Crystal Structure Determination, 2025, DOI: **10.5517/ccdc.csd.cc2nbcds**; (*c*) P. Podchorodecka, B. Dziuk, R. Szostak, M. Szostak and E. Bisz, CCDC 2452826: Experimental Crystal Structure Determination, 2025, DOI: **10.5517/ccdc.csd.cc2nbcft**.

This journal is © The Royal Society of Chemistry 2025